KRUGLOV, M. V., SOZONTOV, E. A., SHCHEMELEV, V. N. & ZAKHAROV, B. G. (1977). *Kristallografiya*, **22**, 693-697.

LAUE, M. VON (1931). *Ergeb. Exakten Naturwiss.* **10**, 133-458.

LAUE, M. VON (1960). *Rontgenstrahl Interferenzen.* Frankfurt am Main: Akademische Verlagsgesellshaft.

PATEL, J. R. & GOLOVCHENKO, J. A. (1983). *Phys. Rev. Lett.* **50**, 1858-1861.

PATEL, J. R., GOLOVCHENKO, J. A., BEAN, J. C. & MORRIS, R. J. (1985). *Phys. Rev. B*, **31**, 6884-6886.

PENNING, P. & POLDER, D. (1961). *Philips Res. Rep.* **16**, 419-440.

PINSKER, Z. G. (1978). *Dynamical Scattering of X-rays in Crystals.* Berlin: Springer.

TAKAHASHI, T. & KIKUTA, S. (1979). *J. Phys. Soc. Jpn*, **47**, 620.

ZACHARIASEN, W. H. (1945). *Theory of X-ray Diffraction in Crystals.* New York: John Wiley.

Acta Cryst. (1986). A42, 426-435

The Dynamical Diffraction of X-ray Spherical Waves in Two Perfect Crystals

BY V. V. ARISTOV AND A. A. SNIGIREV

Institute of Problems of Microelectronic Technology and Superpure Materials, USSR Academy of Sciences, 142432 Chernogolovka, Moscow District, USSR

AND A. M. AFANAS'EV, V. G. KOHN AND V. I. POLOVINKINA

I. V. Kurchatov Institute of Atomic Energy, Moscow 123183, *USSR*

(*Received* 22 *August* 1985; *accepted* 10 *February* 1986)

Abstract

The general theory of X-ray spherical-wave diffraction in two, either identical or different in nature, spatially separated perfect crystals is developed. The theory takes into account the phase shift of the waves both inside the crystals and in vacuum before, between and after the crystals. The nonmonochromaticity of radiation, the source dimension and the placing of a slit before the first crystal are considered. The results of theoretical calculation and an experimental study of the interference fringes and focusing the radiation are presented. A good agreement between the experimental and theoretical data is obtained for values of the experimental parameters that affect focusing.

1. Introduction

The diffraction pattern on the film behind a perfect crystal due to X-ray-spherical-wave diffraction is known (Afanas'ev & Kohn, 1977) to be defined to a great extent by the wave phase change occurring both inside the crystal and in vacuum along the source-crystal-film wave path L. In other words, the form of the diffraction pattern depends on the parameter t/L, where t is the crystal thickness. To observe this dependence experimentally one has to use either monochromatic radiation (Aristov, Ishikawa, Kikuta & Polovinkina, 1981) or a special set-up in which polychromatic focusing is realized (Aristov, Polovinkina, Shmyt'ko & Shulakov, 1978; Kozmik & Mikhailyuk, 1978*a*, *b*; Aristov & Polovinkina, 1978; Aristov, Polovinkina, Afanas'ev & Kohn, 1980). In the above papers all the new details of the diffraction pattern introduced by the theory have been obtained experimentally, namely, focusing of the radiation and the anomalous form of the *Pendellösung* fringes.

The effect of an entrance slit placed in front of the crystal on the diffraction pattern has been investigated in the papers by Aristov, Kohn & Polovinkina (1980) and Aristov, Kohn, Polovinkina & Snigirev (1982). The slit was shown to play the role of an incoherent source when its width $2a$ is much less than either the source dimensions or the 'spectral' width $d_s = (\Gamma/\omega)L_1 \tan\theta_B$, where Γ is the half-width of the spectral line, ω is the radiation frequency, L_1 is the source-to-crystal distance and θ_B is the Bragg angle. This case is realized in standard section topography of the experimental set-up with a narrow slit before the crystal, which is equivalent to the case of a point source on the entrance surface of a crystal (Kato, 1961, 1968).

The present paper is related to a further study of the role of the vacuum in X-ray-spherical-wave diffraction. The Laue diffraction in two perfect crystals has been considered. It is particularly interesting owing to strong focusing occurring in two-block crystals with equal block thickness and $L = 0$. This effect was first seen in the case of a small gap between two identical crystals (Kato, Usami & Katagawa, 1967; Authier, Milne & Sauvage, 1968) when direct and diffracted beams were not spatially separated. In the first paper the stacking fault was used as a gap. The next step was made by Indenbom, Slobodetsky & Truni (1974). The effect was shown to occur also with a large gap between the blocks in the twice-reflected

0108-7673/86/060426-10$01.50

beam (Π-shaped interferometer). This phenomenon has received further experimental study (Suvorov & Polovinkina, 1974; Indenbom & Suvorov, 1976; Indenbom, Suvorov & Slobodetsky, 1976).

In § 2 a general theory for X-ray-spherical-wave diffraction in two perfect crystals is developed. The theory takes into account the path of waves in vacuum and the positioning of a slit before the first crystal as well as the nonmonochromaticity of the radiation and the source dimensions. As in previous papers (Afanas'ev & Kohn, 1977; Aristov, Polovinkina, Afanas'ev & Kohn, 1980), the method of Fourier transformation was applied. General formulae are analysed in § 3. Experimental results are presented in § 4.

2. Derivation of general formulae

Let us consider the experimental set-up shown in Fig. 1. The incident radiation is formed by an incoherent source of finite dimensions and a finite spectral width. In the first stage of the problem we have to obtain the solution for a point source and a specific frequency and then sum the intensity over all frequencies and all coordinates of the atoms at the X-ray tube focus. It is convenient to introduce a coordinate system with origin at the slit-plane centre for all waves. We use a unit vector $\mathbf{S}_0$ in the Bragg direction for the frequency ω_0 corresponding to a maximum of intensity in the spectrum. Then the wave vector is $\boldsymbol{\varkappa}_0 = \varkappa_0 \mathbf{S}_0$, where $\varkappa_0 = \omega_0/c$, c is the light velocity. We present the electric-field amplitude of the X-ray spherical wave in the slit plane as the Fourier integral

$$\mathbf{E}_0^{(\mathrm{in})}(\mathbf{r}) = \sum_s A_s(\omega)\mathbf{e}_{0s} \int \mathrm{d}\mathbf{q}(2\pi)^{-2} \exp(i\mathbf{q}\mathbf{r})\psi(\mathbf{q}), \quad (1)$$

where $\mathbf{q}$ is a vector perpendicular to $\boldsymbol{\varkappa}_0$ (see Fig. 1), $\mathbf{e}_{0s}$ are the unit vectors of polarization, $s = \pi, \sigma$. The function $\psi(\mathbf{q})$ depends on the slit width, radiation frequency and position of the point source on the X-ray tube focus and will be described below. The parameters $A_s(\omega)$ are the coefficients of expansion of the electric field vector on the polarization vectors. They include the frequency dependence of the characteristic radiation within the spectral line.

According to Maxwell's equation in vacuum, the amplitude of the field of frequency ω at the entrance surface of the first crystal is

$$\mathbf{E}_0^{(\mathrm{in})}(\mathbf{r}) = \sum_s A_s(\omega) e_{0s} \times \int \mathrm{d}\mathbf{q}(2\pi)^2 \exp[i\mathbf{K}_0(q)\mathbf{r}]\psi(\mathbf{q}), \quad (2)$$

where

$$\mathbf{K}_0 = \mathbf{q} + \mathbf{S}_0(\varkappa^2 - q^2)^{1/2} \simeq \boldsymbol{\varkappa}_0 + \mathbf{q} + (\Delta\varkappa - q^2/2\varkappa_0)\mathbf{S}_0. \quad (3)$$

Here $\varkappa = \omega/c = \varkappa_0 + \Delta\varkappa$. The terms of order higher than $(q/\varkappa_0)^2$ in the expansion of the square root in (3) can be neglected, since $q/\varkappa_0 \ll 1$. The same holds for $\Delta\varkappa/\varkappa_0$.

The solution of the problem of scattering of a partial plane wave with wave vector $\mathbf{K}_0$ in a perfect crystal is well known (Pinsker, 1978). Using this solution twice, we obtain the following expression for the amplitude of the field in a twice-diffracted beam:

$$\mathbf{E}_{hh}^{(\mathrm{out})}(\mathbf{r}) = \sum_s A_s(\omega)\mathbf{e}_{2s} \int \mathrm{d}\mathbf{q}(2\pi)^{-2}\psi(\mathbf{q}) \times R_s^{(1)}(\mathbf{q})R_s^{(2)}(\mathbf{q}) \exp[i\varphi(\mathbf{q}, \mathbf{r})], \quad (4)$$

where $\mathbf{e}_{2s}$ are polarization vectors for the twice-diffracted wave, $R_s^{(i)}(\mathbf{q})$ is the amplitude of reflection of a plane wave by the perfect crystal [see, for example, formulae (3.10) and (3.11) in the paper by Aristov, Polovinkina, Afanas'ev & Kohn (1980)].

The phase term $\exp(i\varphi)$ accounts for the phase shift of the plane wave with wave vector $\mathbf{K}_0$ between the slit and the first crystal, $\mathbf{K}_1$ between the first and second crystals and $\mathbf{K}_2$ after the second crystal. The wave vectors $\mathbf{K}_1$ and $\mathbf{K}_2$ are determined by the following relations:

$$\begin{aligned} \mathbf{K}_1(\mathbf{q}) &= \mathbf{K}_0(\mathbf{q}) + \mathbf{h}_1 - \alpha_1(\mathbf{q})\mathbf{n}_1/2 \\ \mathbf{K}_2(\mathbf{q}) &= \mathbf{K}_1(\mathbf{q}) + \mathbf{h}_2 - \alpha_2(\mathbf{q})\mathbf{n}_2/2, \end{aligned} \quad (5)$$

where $\mathbf{h}_1, \mathbf{h}_2$ are the reciprocal-lattice vectors and $\mathbf{n}_1, \mathbf{n}_2$ are the inner normals to the entrance surfaces of the first and second crystals. The parameters $\alpha_1(\mathbf{q})$ and $\alpha_2(\mathbf{q})$ are found from the condition that the scattering is elastic (the frequency is constant), *i.e.* $K_2^2 = K_1^2 = K_0^2$, and are calculated in the Appendix.

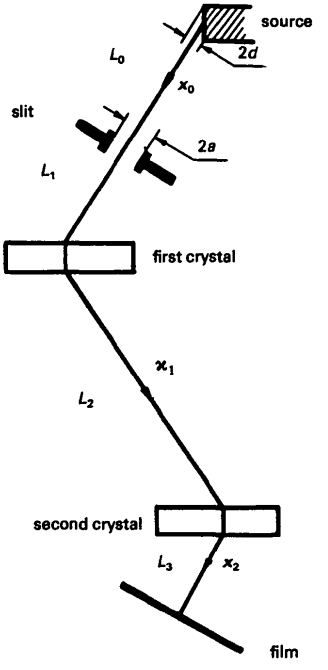

Fig. 1. Experimental set-up.

Let us consider the function $\psi(\mathbf{q})$. According to (1) it is the Fourier component of a scalar amplitude of the electric field in the slit plane, $\psi(\mathbf{r})$. In its turn, $\psi(\mathbf{r})$ is the spherical wave moving from the point source on the focus of the X-ray tube. Without any loss of generality, instead of the real focus surface, we can consider its projection on a plane normal to $\boldsymbol{\varkappa}_0$ (see Fig. 1). Let L_0 be the source-to-slit distance; (x_1, y_1) are the coordinates in the slit plane, (x_0, y_0) are the coordinates in the plane of the focus projection. It is obvious that

$$\psi(\mathbf{r}) = [\exp(i\varkappa R)/R]\theta(a-|x_1|), \tag{6}$$

where $2a$ is the slit width, $\theta(x)$ is the step function which is equal to one for $x>0$ and is equal to zero for $x<0$, $R=|\mathbf{R}|$,

$$\mathbf{R} = L_0\mathbf{S}_0 + (x_1-x_0)\mathbf{e}_{0\pi} + (y_1-y_0)\mathbf{e}_{0\sigma}. \tag{7}$$

Here and below the unit vectors of polarization are chosen as usual, namely, $\mathbf{e}_{n\sigma}$ normal to the scattering plane (plane of Fig. 1), $\mathbf{e}_{n\pi} = [\mathbf{e}_{n\sigma}\times\mathbf{S}_n]$, where $\mathbf{S}_n = \boldsymbol{\varkappa}_n/\varkappa_0$, $n=0,1,2$ (see Appendix for $\boldsymbol{\varkappa}_n$). From (6), (7) we have approximately

$$\begin{aligned}\psi(\mathbf{r}) = {} & [\exp(i\varphi_0)/L_0]\theta(a-|x_1|)\\ & \times\exp[i(\varkappa_0/2L_0)(x_1^2-2x_1x_0)]\\ & \times\exp[i(\varkappa_0/2L_0)(y_1-y_0)^2],\end{aligned} \tag{8}$$

where the phase φ_0 depends on $\Delta\varkappa$ but does not depend on the integration variables (x_1, y_1), and the corresponding phase factor has, therefore, no influence on the intensity. Below we shall omit such factors. The terms of type $\Delta\varkappa x_1^2/2L_0$ are small and can be neglected. We represent the Fourier component of (8) in the following form:

$$\psi(\mathbf{q}) = \psi_1(q_x)\psi_2(q_y), \tag{9}$$

where

$$\begin{aligned}\psi_1(q_x) = {} & L^{-1/2}\int_{-a}^{a} dx_1 \exp(-iq_xx_1)\\ & \times\exp[i(\varkappa_0/2L_0)(x_1^2-2x_1x_0)],\end{aligned} \tag{10}$$

$$\begin{aligned}\psi_2(q_y) = {} & L^{-1/2}\int_{-\infty}^{\infty} dy_1 \exp(-iq_yy_1)\\ & \times\exp[i(\varkappa_0/2L_0)(y_1-y_0)^2]\\ = {} & (2\pi i/\varkappa_0)^{1/2}\exp(-iq_yy_0 - iq_y^2L_0/2\varkappa_0).\end{aligned} \tag{11}$$

With (11) and the fact that $R_s^{(i)}$ does not depend on q_y, the integral over q_y in (4) can be easily computed. Indeed, as is shown in the Appendix, the phase shift

$$\varphi(\mathbf{q},\mathbf{r}) = \tilde{\varphi}(q_x) + q_xx + q_yy - q_y^2L/2\varkappa_0,$$

where x, y are the coordinates in the film plane along the $\mathbf{e}_{2\pi}$ and $\mathbf{E}_{2\sigma}$ directions, L is the slit-first-crystal-second-crystal-film distance ($L = L_1+L_2+L_3$, see Fig. 1). Therefore, the integral over q_y is

$$\begin{aligned}&\int_{-\infty}^{\infty} dq_y(2\pi)^{-1}(2\pi i/\varkappa_0)^{1/2}\\ &\quad\times\exp[iq_y(y-y_0)]\exp[-i(q_y^2/2\varkappa_0)(L_0+L)]\\ &\quad = (L+L_0)^{-1/2}\exp\{i[\varkappa_0/2(L+L_0)](y-y_0)^2\}.\end{aligned} \tag{12}$$

Thus, the y dependence of the spherical wave is conserved in the diffraction process, but the decrease in intensity from this component is due to the total source-to-film distance.

As a result, instead of (4), omitting the phase factors we obtain

$$\begin{aligned}\mathbf{E}_{hh}^{(\mathrm{out})}(x) = {} & \sum_s A_s(\omega)\mathbf{e}_{2s}(L+L_0)^{-1/2}\\ & \times\int_{-a}^{a} dx_1\,\psi_1(x_1)F^{(s)}(x-x_1),\end{aligned} \tag{13}$$

where

$$\begin{aligned}F_{(x)}^{(s)} = {} & \int_{-\infty}^{\infty} dq_x(2\pi)^{-1}R_s^{(1)}(q_x)R_s^{(2)}(q_x)\\ & \times\exp[iq_xx + i\tilde{\varphi}(q_x)].\end{aligned} \tag{14}$$

Formulae (13) and (14) represent the solution of the problem, but are not suitable for practical calculation or qualitative analysis.

Let us introduce the angle of misorientation between the crystals ψ_h and proceed with (14) to a new integration variable

$$q = q_x - \tan\theta_B^{(1)}\Delta\varkappa - q_0, \tag{15}$$

where

$$\begin{aligned}&q_0 = (\pi/\lambda)[D\theta_\omega + \psi_h],\\ &\theta_\omega = \Delta\varkappa/\varkappa,\\ &D = \sin(\theta_B^{(1)} - \theta_B^{(2)})/\cos\theta_B^{(1)}\cos\theta_B^{(2)}.\end{aligned} \tag{16}$$

It should be emphasized that the reflection amplitude $R_s^{(i)}$ depends on the parameter $y_i^{(s)}$ only [see formulae (3.10), (3.11) in the paper by Aristov, Polovinkina, Afanas'ev & Kohn (1980)]. Using a new variable we obtain for symmetrical scattering in both crystals ($\mathbf{h}\perp\mathbf{n}$)

$$y_1^{(s)} = \Lambda_1^{(s)}(q+q_0),\ y_2^{(s)} = \Lambda_2^{(s)}(-q+q_0), \tag{17}$$

where

$$\Lambda_i^{(s)} = (\lambda/2\pi)\sin 2\theta_B^{(i)}/|\chi_{rh}^{(i)}|c_s^{(i)}.$$

Here and above θ_B is the Bragg angle, χ_{rh} is the Fourier component of the real part of the polarizability, c_s is equal to unity for $s=\sigma$ and $\cos 2\theta_B$ for $s=\pi$, index i is the crystal number and λ is the wavelength of radiation.

It follows from (17) that the parameter q is an angle variable when the radiation has frequency ω_0 and there is no misorientation between the crystals ($\theta_\omega = \psi_h = 0$). If $\theta_\omega \neq 0$, but $D = 0$ ($\theta_B^{(1)} = \theta_B^{(2)}$), then y_1 and y_2 do not depend on θ_ω, and parameter q is the same for all frequencies. It can be shown that (see Appendix)

$$\tilde{\varphi}(q) = \Delta\varphi + x_c q - (\lambda L/4\pi)q^2 + q(t_1 \sin\theta_B^{(1)} - t_2 \sin\theta_B^{(2)}) - \alpha_1(q)t_{1/2} - \alpha_2(q)t_2/2. \quad (18)$$

Here $\Delta\varphi$ denotes all the terms that are independent of q; t_1 and t_2 are the crystal thicknesses. The last four terms are cancelled out by the corresponding terms in the phases of the amplitudes $R^{(i)}(y_i^{(s)})$. The value of x_c is

$$x_c = -\tfrac{1}{2}L\psi_h + \Delta L\theta_\omega, \quad (19)$$

where

$$\Delta L = \tan\theta_B^{(1)}(L_2 - L_1 - L_3) - \tfrac{1}{2}D(L_1 + L_2 - 3L_3). \quad (20)$$

The topography fixes the intensity of radiation, which is equal to the squared modulus of the electric-field amplitude (13). Since the spectrum of incident radiation has, as a rule, finite width and the source has finite dimensions, the intensity integrated over the source dimensions $2d$ is of interest as well as that integrated over the spectral width of radiation. We must also average the intensity over the polarization state of the incident waves, *i.e.* parameters $|A_s(\omega)|^2$. The corresponding value $\xi(\theta_\omega) = 2|A_s(\omega)|^2$ characterizes the form of the spectral line of the source. As a result, we obtain

$$\bar{I}_{hh}(x) = [2L_0(L_0+L)]^{-1} \sum_s \int_{-\infty}^{\infty} d\theta_\omega \xi(\theta_\omega) \times \int_{-d}^{d} dx_0 \left| \int_{-a}^{a} dx_1 G_\omega^{(s)}(x - x_1) \times \exp[i(\pi/\lambda L_0)(x_1^2 - 2x_1x_2)] \right|^2. \quad (21)$$

Here the explicit form of the function $\psi_1(q_x)$ following from (10) was used and $x_2 = x_0 + L_0\theta_\omega(\tan\theta_B^{(1)} + \frac{1}{2}D) + \frac{1}{2}L_0\psi_h$, while the function $G_\omega^{(s)}(x)$ differs from $F_\omega^{(s)}(x)$ only by the phase factors.

Taking into account the expression for $R(y)$, we obtain

$$G_\omega^{(s)}(x) = (8\pi)^{-1}(\chi_h^{(1)}\chi_h^{(2)}/\chi_{\bar{h}}^{(1)}\chi_{\bar{h}}^{(2)})^{1/2} \sum_{j,j'} z_j z_{j'} \times \int_{-\infty}^{\infty} dq \exp[iqx + i\varphi_{jj'(q)}^{s\omega} - f_{jj'}^{sw}(q)], \quad (22)$$

where

$$\varphi_{jj'}^{sw}(q) = x_c q - (\lambda L/4\pi)q^2 + z_j B_1(q)(\sin\theta_B^{(1)}/\Lambda_1)t_1 + z_{j'}B_2(q)(\sin\theta_B^{(2)}/\Lambda_2)t_2, \quad (23)$$

$$f_{jj'}^{sw}(q) = \mu_{sj}^{(1)}(q)t_1 + \mu_{sj'}^{(2)}(q)t_2 + \ln[B_1(q)B_2(q)] \quad (24)$$

$$B_i(q) = [1 + y_i^2(q)]^{1/2}, \qquad i = 1, 2, \quad (25)$$

$$\mu_{sj}^{(i)}(q) = [\mu_0^{(i)}/2\cos\theta_B^{(i)}][1 - z_j|\chi_{ih}^{(i)}|C_s^{(i)}/\chi_{i0}^{(i)}B_i(q)]. \quad (26)$$

Here indexes $j, j' = 1, 2$ are the numbers of the dispersion surface branch, $\mu_0^{(i)}$ is the normal absorption coefficient for the ith crystal, z_j is $+1$ for $j = 1$ (a weakly absorbing branch) and -1 for $j = 2$, $\chi_{i0}^{(i)}$, $\chi_{ih}^{(i)}$ are the imaginary parts of the Fourier transforms of the polarizability of the ith crystal.

It is obvious that if two crystals are identical ($\theta_B^{(1)} = \theta_B^{(2)}$), then the function $G_\omega^{(s)}(x)$ does not depend on frequency under certain conditions, but if the crystals are different the dependence is preserved under any condition.

The case when the distance L_0 is relatively small while the source dimensions exceed the slit width considerably is of particular interest. With reasonable accuracy one may use here the approximation

$$\int_{-d}^{d} dx_0 \exp[i(2\pi/\lambda L_0)(x_1 - x_1')x_0] \simeq \lambda L_0 \delta(x_1 - x_1'). \quad (27)$$

As a result, instead of (21) (*cf.* Aristov *et al.*, 1982) we obtain

$$\bar{I}_{hh}(x) = [\lambda/2(L+L_0)^2] \times \sum_s \int_{-\infty}^{\infty} d\theta_\omega \xi(\theta_\omega) \int_{-a}^{a} dx_1 |G_\omega^{(s)}(x - x_1)|^2. \quad (28)$$

It follows from (28) that the x dependence of the intensity is determined as if the slit itself were an 'incoherent' source. Except for the trivial factor there is no dependence on L_0 here.

3. Interference effects and focusing the spherical wave

According to (28) the space dependence of intensity in the twice-reflected beam is determined by the squared modulus of the function $G(x)$. The integration with respect to the slit width and frequency plays only a destructive role changing the interference contrast for the worse. Let us consider first the simplest case when the slit may be regarded as rather narrow, and the first and second crystals are identical without any misorientation between them ($\psi_h = 0$, $\Lambda_1 = \Lambda_2 = \Lambda$, $B_1 = B_2 = B$ *etc.*). Since the dependence on frequency occurs in (25) only through the coordinate

x_c [see (19)] it is easy to understand that the integration with respect to the frequency leads to blurring of the interference pattern in the same manner as the integration over the slit width. However, the degree of blurring depends on the parameters of the experimental set-up. When $L_2 = L_1 + L_3$ polychromatic focusing exists, and the nonmonochromaticity of the radiation does not influence the interference pattern. We shall consider this condition as fulfilled.

For usual values of L, t_1 and t_2, phase (23) is rather large and integral (22) can be evaluated by the method of stationary phase (Jeffreys & Swirles, 1966). As a result

$$I_{hh}(x) = |G(x)|^2 \simeq \tfrac{1}{4}|\chi_h/\chi_{\bar{h}}|^2 \left| \sum_{jj'} z_j z_{j'} \times \frac{\exp[iqx + i\varphi_{jj'}(q) - f_{jj'}(q)]}{(\mathrm{d}^2\varphi_{jj'}/\mathrm{d}q^2)^{1/2}} \right|^2, \quad (29)$$

where q is found from the condition

$$x = (\lambda L/2\pi)q - \sin\theta_B \Lambda [q/B(q)]t. \quad (30)$$

Here and below $t = z_j t_1 + z_{j'} t_2$. A second derivative of the phase has the following form:

$$\mathrm{d}^2\varphi_{jj'}/\mathrm{d}q^2 = -\mathrm{d}x/\mathrm{d}q = -\lambda L/2\pi + \sin\theta_B \Lambda t/B^3(q). \quad (31)$$

From the condition that the above derivative equals zero we find the locus of the focuses

$$x = \pm t[1 - (t_s/t)^{2/3}]^{3/2} \sin\theta_B. \quad (32)$$

These formulae coincide precisely with the formulae obtained by Aristov, Polovinkina, Afanas'ev & Kohn (1980), and the parameter t_s has the same sense. It represents the focusing thickness for one crystal and is given by

$$t_s = \lambda L/2\pi \sin\theta_B \Lambda, \quad (33)$$

while the parameter t has a new meaning and only $t > 0$ should be considered in (32).

The value of the angle variable q, which determines the focusing region of angles, is also an important characteristic:

$$q = \pm \Lambda^{-1}[(t/t_s)^{2/3} - 1]^{1/2}. \quad (34)$$

It follows from (34) that the strongest focusing occurs at $t = t_s$ corresponding to the point $q = 0$. Let us, as in the works by Aristov, Kohn & Polovinkina (1980) and by Kohn (1979*a*, *b*), call the fields corresponding to a weakly absorbing and a strongly absorbing mode the B field ($j = 1$) and the A field ($j = 2$), respectively.

The following combinations for the crystal thicknesses are possible:

1. $t_1 + t_2 = t_s$ the focusing of the BB field
2. $t_1 = t_2 + t_s$ the focusing of the BA field
3. $t_1 = t_2 - t_s$ the focusing of the AB field.

It should be noted that in the short report by Levonyan (1981) only the first and the third cases were shown while considering an analogous problem. The first is trivial in the sense that two crystals act as a single one of total thickness. The second and third possibilities are new. It is easily seen that these two possibilities are also realized for $L = 0$ ($t_s = 0$). In this case two of the four fields (BA and AB) are brought into focus for the same relationship between the crystal thicknesses: $t_1 = t_2$, and the decrease of the total intensity occurs with the normal absorption factor. A fascinating property of focusing at $L = 0$ is that not only the second derivative of the phase becomes zero, but also the whole phase equals zero. For weakly absorbing crystals the intensity at the focus is very high in this case. Such focusing was first predicted by Indenbom, Slobodetsky & Truni (1974) using the influence function.

With increasing distance L the relationship between the crystal thicknesses for BA and AB fields becomes different. If the first crystal has a variable thickness (when cut as a wedge) and $t_2 > t_s$, there are two focuses, $t_1 = t_2 \pm t_s$, on the plane (x, t_1). Fig. 2 shows the intensity $I_{hh}(x, t_1)$ calculated using (29) for two silicon crystals, Au $L\alpha$ radiation ($\lambda = 1{\cdot}276$ Å), reflection 220, $t_2 = 124$ μm, $L = 1$ cm ($t_s \simeq 0$, Fig. 2*a*) and $L = 140$ cm ($t_s = 42{\cdot}1$ μm, Fig. 2*b*). It should be noted that Fig. 2 presents only the central part of the

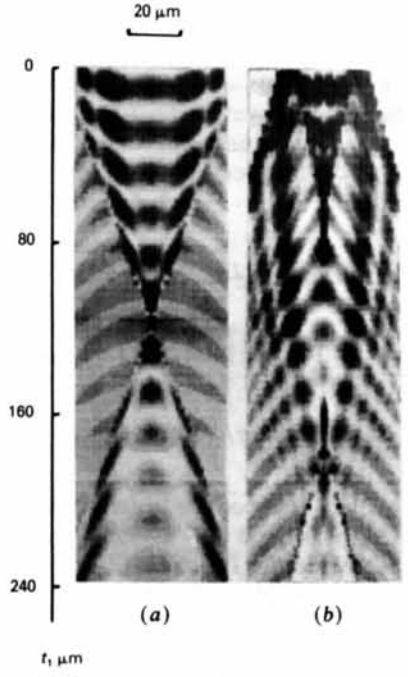

Fig. 2. Theoretical topographs of Si–Si crystals in twice-reflected beam. Reflections 220/220; Au $L\alpha$ radiation ($\lambda = 1{\cdot}276$ Å). The first crystal is cut as a wedge, thickness of the second crystal $t_2 = 124$ μm, source-to-film distance $L = 1$ cm (*a*) and $L = 140$ cm (*b*). (*a*) $t_s = 0$; $t_{1f}^{BA} = t_{1f}^{AB} = t_2 = 124$ μm. (*b*) $t_s = 41{\cdot}2$ μm; $t_{1f}^{BA} = 166{\cdot}1$ μm; $t_{1f}^{AB} = 82{\cdot}9$ μm.

topographs. The real width of the topographs depends on t_1 and is wider than in Fig. 2. These figures indicate that the effect of focusing is accompanied by a rather complicated structure of interference fringes, the interference pattern getting much more diversified with increasing source-to-film distance L due to the foci splitting.

To gain a better insight into the structure of the pictures shown in Fig. 2 let us consider conditions for focusing of the non-central part of the angles ($q \neq 0$). According to (34) this condition is $t > t_s$. On conversion to the thickness of the first crystal it means:

1. $t_1 > t_s - t_2$ *BB* field
2. $t_1 > t_2 + t_s$ *BA* field
3. $t_1 < t_2 - t_s$ *AB* field.

Thus, in the first and second instances caustics $x_{cau}(t_1)$ are directed toward the acute part of the wedge (toward the smaller thicknesses), while in the third instance they are in the opposite direction.

By analysing phase diagrams as for one crystal (Aristov, Polovinkina, Afanas'ev & Kohn, 1980) it is possible to show that the points of the stationary phase in the central portion of the angles ($q = 0$) exist only for the values of x that satisfy the condition $|x| < |x_{cau}|$. Therefore, the intensity of any of the four fields in the region of thickness t_1, where caustics exist, is concentrated only between them. This condition permits the classification of the form of the fringes observed. Bright interference fringes in the upper part of Fig. 2(a) (the region of small thicknesses) correspond to the intereference of *BB* and *AB* fields and those in the lower part to the interference of *BA* and *AA* fields. The interference fringes of low contrast in the region $|x| > |x_{cau}|$ are due to the interaction between *BB* and *AA* fields because *AB* and *BA* fields make practically no contribution to this region. These fringes have a form that corresponds to a 'virtual' focus of the *BB* field in the region of negative thicknesses of the first crystal.

The fringes in Fig. 2(b) may be classified in the same way. In this case the virtual focus is situated closer to the point $t_1 = 0$, and the caustics of the *BB* field are easily seen in the upper part of the topographs. On the contrary, the caustics corresponding to the focusing of the *BA* field show themselves weakly. The splitting of the foci corresponding to *BA* and *AB* fields is also visible.

Let us consider now a more complicated situation when two crystals are different but have similar structures, using the reflection from the same set of planes. From the experimental point of view it is convenient to use germanium as the first crystal and silicon as the second one. Since the difference between the lattice constants of these crystals is small, the value of $\sin\theta_B^{(1)}$ is close to $\sin\theta_B^{(2)}$. Therefore, the parameter D is not equal to zero but is small, and the dependence on frequency appearing in Green's function (22) proved to be weak within the spectral line width, and the nonmonochromaticity does not influence the contrast very much. It should be emphasized that for this reason it is impossible to realize experimentally the focusing of X-rays on two crystals when using reflections from different sets of planes without pre-monochromatization of the radiation.

In the case under consideration, (29) remains unchanged, but instead of (30) and (31) we obtain, respectively

$$x + x_c = (\lambda L/2\pi)q - z_j t_1[\Lambda_1(q+q_0)/B_1(q)]\sin\theta_B^{(1)} - z_{j'} t_2[\Lambda_2(q-q_0)/B_2(q)]\sin\theta_B^{(2)} \quad (35)$$

$$d^2\varphi_{jj'}/dq^2 = -dx/dq = -\lambda L/2\pi + z_j t_1[\Lambda_1/B_1^3(q)]\sin\theta_B^{(1)} + z_{j'} t_2[\Lambda_2/B_2^3(q)]\sin\theta_B^{(2)}. \quad (36)$$

The caustics $x_{cau}(t_1)$ can be determined from the condition that (36) equals zero. To do this, it is necessary to find from (36) the appropriate value of q, which depends on L, t_1, t_2, and substitute it into (35).

However, this problem has no analytical solution for any value of q. Therefore, from now on we shall restrict ourselves to monochromatic radiation ($\theta_\omega = 0$) and small values of q. As before, we assume that $\psi_h = 0$. In the region $|q| \ll \Lambda^{-1}$ we obtain

$$q^2 = \frac{2}{3}\frac{(z_j T_1 + z_{j'} T_2 - 1)}{\Lambda_1^2 + z_{j'} T_2(\Lambda_2^2 - \Lambda_1^2)}, \qquad T_i = \frac{t_i}{t_s^{(i)}}, \quad (37)$$

where the parameter $t_s^{(i)}$ is determined by (33) and refers to the ith crystal. In the vicinity of the diffraction-pattern centre we obtain

$$x_{cau}(t_1) \simeq \pm(\tfrac{2}{3})^{3/2} t_s^{(1)} \sin\theta_B^{(1)} \times\{1 + z_{j'} T_2[(\Lambda_2/\Lambda_1)^2 - 1]\}^{-1/2} \times (z_j T_1 + z_{j'} T_2 - 1)^{3/2}. \quad (38)$$

With identical crystals (37) and (38) correspond to the first terms in the expansion of (32) and (34) into a power series of a small parameter $(t/t_s - 1)$.

According to the expressions obtained, the focusing of the central region occurs under the condition $t_1 = z_j t_s^{(1)} - z_j z_{j'} t_2 K_{12}$, where $K_{12} = t_s^{(1)}/t_s^{(2)}$ does not depend on L. From the expression for t_1 and with (38) we obtain for individual fields:

1. $t_1 \geq t_s^{(1)} - t_2 K_{12}$ the focusing of the *BB* field
2. $t_1 \geq t_2 K_{12} + t_s^{(1)}$ the focusing of the *BA* field
3. $t_1 \leq t_2 K_{12} - t_s^{(1)}$ the focusing of the *AB* field.

The presence of K_{12} in the inequalities results in essential differences compared to the above case of two identical crystals. Even at $L = 0$ the focusing occurs with different crystal thicknesses. For the Ge/Si combination (reflection 111, Au $L\alpha$ spectral line), $K_{12} = 2{\cdot}50$ for σ polarization. This results in a

considerable enhancement of the focusing thickness t_{1f}^{BA} for the *BA* field and many anomalous *Pendellösung* fringes are observed in the region $t_1 < t_{1f}^{BA}$ (Aristov, Polovinkina, Afanas'ev & Kohn, 1980). The second crystal plays the same role as the source-to-film distance. Fig. 3(*a*) shows the interference pattern calculated from (29), (35) and (36) for σ polarization and $t_2 = 50$ μm, $L = 40$ cm. Here $t_{1f}^{BA} = 191$ μm, while $t_s^{(1)} = 65{\cdot}8$ μm and the extinction length $L_{ex}^{(1)} = \pi\Lambda_1 \sin\theta_B^{(1)} = 10{\cdot}2$ μm (Aristov, Polovinkina, Afanas'ev & Kohn, 1980). The anomalous *Pendellösung* fringes, which are due to the interference of *BA* and *AA* fields, can be seen in the figure (in the region of small values of t_1). The caustics of the *BB* field are also easily seen. Fig. 3(*b*) is the same but for unpolarized radiation. As illustrated, the superposition of different polarizations leads to a deterioration of the contrast. The main cause of this is the difference in the extinction lengths and in the focusing thicknesses for the two polarizations.

4. Experimental results

Experimental studies were carried out according to the scheme of Fig. 1. A microfocus X-ray generator Microflex (Rigaku Denki) with a focus size not greater than 10×10 μm served as a radiation source. The slit placed before the first crystal had a width of more than 100 μm and served simply for the separation of the Au $L\alpha_1$ spectral line with $\lambda = 1{\cdot}276$ Å. Thus, approximation (27) is inapplicable to these experimental conditions and instead of (28) it is necessary to use formula (21) in which the limits $\pm a$ can be replaced by $\pm\infty$. Taking into account the explicit expression for Green's function (22), one can easily show that (28) is valid again, if a is replaced by d (Fig. 1), L_1 by $L_0 + L_1$ and $L_0 = 0$.

The parameters of the experimental set-up were as follows: $L_0 + L_1 = 19$, $L_2 = 20$, $L_3 = 1$ cm. The film was placed just behind the second crystal to permit the reflected–transmitted beam to be recorded simultaneously with the twice-reflected one. The shape and position of the crystals relative to the X-ray beam are shown in Fig. 4. The employment of wedge-shaped crystals made it possible, on the one hand, to observe the diffraction images corresponding to various thicknesses of the first crystal in a topograph and, on the other, to vary the thickness of the second crystal by moving it. Since the wedge angle of the second crystal was small (~2°), the latter might be regarded as plane parallel within the beam range. For obtaining the topographs we use nuclear emulsion plates. The exposure time varied from some tens of minutes up to several hours. Steps have been taken to ensure the stability of the experimental set-up including the mechanical stability during exposure.

The following combinations of crystals and reflections were studied: Si/Si 111, Si/Si 220, Ge/Ge 111, Ge/Si 111. We have also obtained images of two silicon crystals using 220 and 111 reflections for the first and second crystals, respectively. In this case, in full accordance with theoretical results, we observed integral patterns that were highly blurred owing to the nonmonochromaticity of the radiation. In other cases the patterns observed turned out to be very sensitive to crystal misorientation.

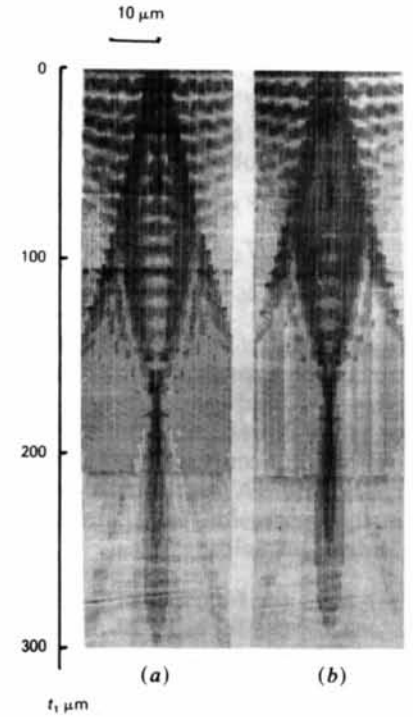

Fig. 3. Theoretical topographs of two crystals in twice-reflected 220/220 beam. Au $L\alpha$ radiation ($\lambda = 1{\cdot}276$ Å). The first crystal (Ge) is cut as a wedge. The second is Si with thickness $t_2 = 50$ μm. The source-to-film distance $L = 40$ cm; $t_s^{(1)} = 65{\cdot}8$ μm; $t_{1f}^{BA} = 191$ μm; $t_{1f}^{AB} = 59{\cdot}2$ μm. (*a*) σ polarization; (*b*) unpolarized radiation.

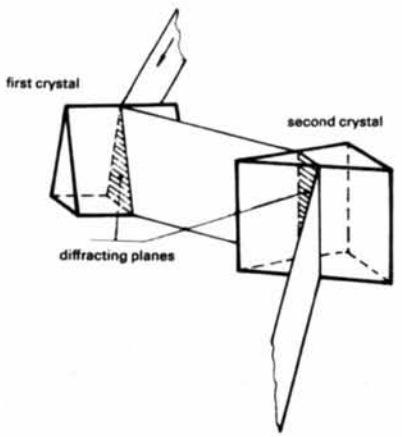

Fig. 4. Position of crystals and reflection planes in the experiment.

The deviation of the second crystal from the exact Bragg position by several seconds results in the reconstruction of the whole pattern, *i.e.* the topograph shows two images in the direct beam as well as in the reflected one. One of these images formed, for example, by the first crystal is transmitted by the second one with small distortions. The topograph shown in Fig. 5 for the Ge/Ge combination of crystals in the 111 reflection at $t_2 = 100$ μm is a typical example.

The best pattern to observe focusing was obtained for the combination Ge/Si 111 at $t_2 = 50$ μm. As has been noted above, the focusing of *AB* and *BA* fields occurs in this case at the thicknesses of the first crystal $t_{1f}^{AB} = 59$ and $t_{1f}^{BA} = 191$ μm. Fig. 6 shows a series of fragments of a diffraction pattern in the twice-reflected beam. The decrease in the pattern width is easily seen in the region of thicknesses close to t_{1f}. In the region between focuses the diffraction line is split into two. This phenomenon is also in good agreement with the theory (see Fig. 3). Unfortunately, the fine structure of the pattern (the anomalous *Pendellösung* fringes, in particular) is not seen in the photograph. This can be explained by the finite dimensions of the X-ray tube focus and possibly by some residual misorientation of the crystals.

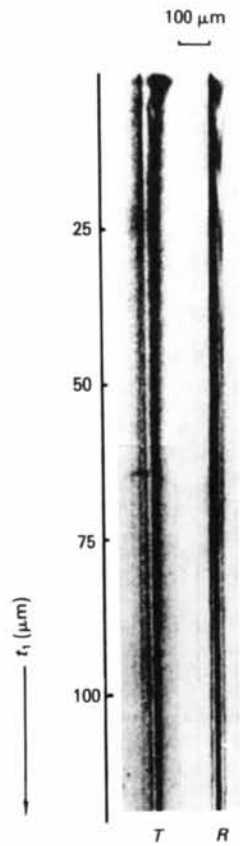

Fig. 5. Experimental topographs for the case of misoriented Ge crystals, *R* is the twice-reflected beam, *T* is the beam reflected by the first crystal and then transmitted by the second one.

5. Concluding remarks

The theoretical and experimental results obtained indicate a significant effect of the phase shift in vacuum on the formation of interference patterns under conditions of X-ray spherical-wave diffraction in two crystals. The diffraction pattern has in this case rather a complicated structure with a wide set of caustics and interference fringes which are due to the interference of various fields in crystals. The lattice distortions will evidently exert different effects on individual fragments of the topograph, and the nature of the defects can be defined by this influence. Thus, the effect of diffraction in two crystals can be used as a new method of control over crystal structure perfection.

It might be well to point out the important advantage of the scheme considered over the Π-shaped interferometer (Bonse, 1975; Bauspiess, Bonse & Graeff, 1976; Indenbom *et al.*, 1974; Suvorov &

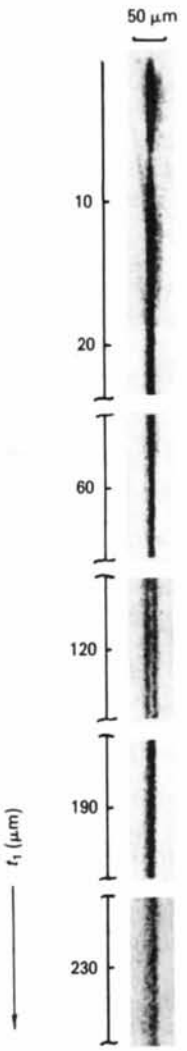

Fig. 6. Set of fragments of experimental topograph corresponding to the case of Fig. 3.

Polovinkina, 1974; Indenbom & Suvorov, 1976; Indenbom *et al.*, 1976). If two arms in this interferometer are in fact parts of the same crystal, the two crystals in our scheme are spatially separated and, moreover, may differ in atomic composition. In doing so, it is appropriate to use the first crystal as a standard and the second one as a specimen under study. To observe the focusing, of great importance also is the scheme stability which is better than that of a Π-shaped interferometer, where even a small variation in the thickness of the arms reduces the effect sharply.

The necessity to adjust the second crystal precisely with respect to the first one seems to be the weakest point of the new scheme. But this difficulty is not a matter of principle and can be solved in the course of further improvements in the set-up. Overall, we conclude that the phenomena discussed are worthy of notice from the standpoints of science and practical considerations.

APPENDIX

For finding the parameters $\alpha_1(\mathbf{q})$ and $\alpha_2(\mathbf{q})$ in (5) and the phase shift $\varphi(\mathbf{q},\mathbf{r})$ in (4) we use three sets of vectors: $\varkappa_n$, $\mathbf{Q}_n$ and $\mathbf{f}_n$, $n=0,1,2$. The vectors $\varkappa_0$, $\varkappa_1$ and $\varkappa_2$ satisfy exactly the Bragg condition for the incident, diffracted and twice-diffracted plane wave with frequency ω_0, $\varkappa_2^2=\varkappa_1^2=\varkappa_0^2$. The vectors $\mathbf{Q}_n$ and $\mathbf{f}_n$ are the linear and square terms in the expansion for a small difference between $\mathbf{K}_n$ and $\varkappa_n$ through terms of order $q/\varkappa_0$. For the corresponding terms in the expansion for $\alpha_n(\mathbf{q})$ the notations $\alpha_n^{(1)}(\mathbf{q})$ and $\alpha_n^{(2)}(\mathbf{q})$ are used. We obtain the following recurrent relations:

$$\begin{aligned}
&\mathbf{Q}_0=\mathbf{q}+\Delta\varkappa\mathbf{S}_0, \quad \mathbf{f}_0=-(q^2/2\varkappa_0)\mathbf{S}_0,\\
&\varkappa_1=\varkappa_0+\mathbf{h}_1, \quad \mathbf{Q}_1=\mathbf{Q}_0-\alpha_1^{(1)}\mathbf{n}_1/2,\\
&\alpha_1^{(1)}=2(\mathbf{h}_1\mathbf{Q}_0)/(\varkappa_1\mathbf{n}_1), \quad \mathbf{f}_1=\mathbf{f}_0-\alpha_1^{(2)}\mathbf{n}_1/2,\\
&\alpha_1^{(2)}=[Q_1^2-Q_0^2+2(\mathbf{h}_1\mathbf{f}_0)]/(\varkappa_1\mathbf{n}_1),\\
&\varkappa_2=\varkappa_1+\mathbf{h}_2^0, \quad \mathbf{h}_2=\mathbf{h}_2^{(0)}+\Delta\mathbf{h}_2,\\
&\mathbf{Q}_2=\mathbf{Q}_1+\Delta\mathbf{h}_2-\alpha_2^{(1)}\mathbf{n}_2/2, \quad \mathbf{f}_2=\mathbf{f}_1-\alpha_2^{(2)}\mathbf{n}_2/2,\\
&\alpha_2^{(1)}=2[(\mathbf{h}_2^{(0)}\mathbf{Q}_1)+(\varkappa_2\Delta\mathbf{h}_2)]/(\varkappa_2\mathbf{n}_2),\\
&\alpha_2^{(2)}=[Q_2^2-Q_1^2+2(\mathbf{h}_2^{(0)}\mathbf{f}_1)]/(\varkappa_2\mathbf{n}_2).
\end{aligned} \tag{A.1}$$

We have introduced here vector $\mathbf{h}_2^{(0)}$, which corresponds to the exact Bragg position of the second crystal with respect to the first one. The second crystal can be removed from this position by simple rotation and, as a result, vector $\mathbf{h}_2$ cannot be coincident with $\mathbf{h}_2^{(0)}$. But only of interest is the case when the angle of rotation is rather small and the ratio $|\Delta\mathbf{h}_2|/\varkappa_0$ is, thus, of the same order of magnitude as the ratio $(q/\varkappa_0)$. Formulae (A.1) are convenient because they are easily generalized to three or more crystals (Kohn, 1979*a*).

The phase shift $\varphi(\mathbf{q},\mathbf{r})$ is determined by the following expression:

$$\varphi(\mathbf{q},\mathbf{r})=\mathbf{K}_0(\mathbf{q})\mathbf{r}_1+\mathbf{K}_1(\mathbf{q})(\mathbf{r}_2-\mathbf{r}_1)+\mathbf{K}_2(\mathbf{q})(\mathbf{r}-\mathbf{r}_2), \tag{A.2}$$

where the vectors $\mathbf{K}_n$ can be written in the form

$$\mathbf{K}_n(\mathbf{q})=\varkappa_n+\mathbf{Q}_n(\mathbf{q})+\mathbf{f}_n(\mathbf{q}). \tag{A.3}$$

If we take (see Fig. 1)

$$\mathbf{r}_1=L_1\mathbf{S}_0, \qquad \mathbf{r}_2=\mathbf{r}_1+\mathbf{n}_1t_1+L_2\mathbf{S}_1,$$
$$\mathbf{r}=\mathbf{r}_2+\mathbf{n}_2t_2+L_3\mathbf{S}_2+x\mathbf{e}_{2\pi}+y\mathbf{e}_{2\sigma}$$

and use (A.1) and (A.2), then we obtain

$$\begin{aligned}
\varphi(\mathbf{q},\mathbf{r})=\varkappa L&+(\mathbf{s}_0\mathbf{f}_0)L_1+(\mathbf{s}_1\mathbf{f}_1)L_2+(\mathbf{s}_2\mathbf{f}_2)L_3\\
&+(\mathbf{K}_1\mathbf{n})t_1+(\mathbf{K}_2\mathbf{n}_2)t_2+\mathbf{Q}_2\mathbf{e}_{2\pi})x+(\mathbf{Q}_2\mathbf{e}_{2\sigma})y.
\end{aligned} \tag{A.4}$$

It is easy to see that $\mathbf{Q}_2\mathbf{e}_{2\sigma}=q_y$ and $(\mathbf{S}_n\mathbf{f}_n)=F_n(q_x)-q_y^2/2\varkappa_0$. Therefore, q_y dependence has the same form as given in the text. The direct calculation in the symmetrical case ($\mathbf{h}\perp\mathbf{n}$) gives $(\mathbf{Q}_2\mathbf{e}_{2\pi})=q_x-2D\Delta\varkappa$, where D is determined by (16). Formulae (17) and (18) can be obtained in the same way. It should also be noted that

$$\begin{aligned}
y_i^{(s)}(qx)&=\alpha_i^{(1)}(q_x)(\varkappa_i\mathbf{n}_i)/2|\chi_{rh}^{(i)}|C_s^{(i)},\\
\Delta\mathbf{h}_2&=|\mathbf{h}_2^{(0)}|\mathbf{n}_2\psi_h.
\end{aligned} \tag{A.5}$$

References

AFANAS'EV, A. M. & KOHN, V. G. (1977). *Fiz. Tverd. Tela*, **19**, 1775-1783.

ARISTOV, V. V., ISHIKAWA, T., KIKUTA, S. & POLOVINKINA, V. I. (1981). *Jpn. J. Appl. Phys.* **20**, 1947-1953.

ARISTOV, V. V., KOHN, V. G. & POLOVINKINA, V. I. (1980). *Phys. Status Solidi A*, **62**, 431-440.

ARISTOV, V. V., KOHN, V. G., POLOVINKINA, V. I. & SNIGIREV, A. A. (1982). *Phys. Status Solidi A*, **72**, 483-491.

ARISTOV, V. V. & POLOVINKINA, V. I. (1978). *Acta Cryst.* A**34**, S227.

ARISTOV, V. V., POLOVINKINA, V. I., AFANAS'EV, A. M. & KOHN, V. G. (1980). *Acta Cryst.* A**36**, 1002-1013.

ARISTOV, V. V., POLOVINKINA, V. I., SHMYT'KO, I. M. & SHULAKOV, E. V. (1978). *Pis'ma Zh. Eksp. Teor. Fiz.* **28**, 6-9.

AUTHIER, A., MILNE, A. D. & SAUVAGE, N. (1968). *Phys. Status Solidi*, **26**, 469-484.

BAUSPIESS, W., BONSE, U. & GRAEFF, W. (1976). *J. Appl. Cryst.* **9**, 68-72.

BONSE, U. (1975). International Summer School on X-ray Dynamical Theory and Topography, Limoges, France, Abstract A9.

INDENBOM, V. L., SLOBODETSKY, I. S. & TRUNI, K. G. (1974). *Zh. Eksp. Teor. Fiz.* **66**, 1110-1120.

INDENBOM, V. L. & SUVOROV, E. V. (1976). *Pis'ma Zh. Eksp. Teor. Fiz.* **23**, 485-489.

INDENBOM, V. L., SUVOROV, E. V. & SLOBODETSKY, I. S. (1976). *Zh. Eksp. Teor. Fiz.* **71**, 359-369.

JEFFREYS, H. & SWIRLES, B. (1966). *Methods of Mathematical Physics*. Cambridge Univ. Press.

KATO, N. (1961). *Acta Cryst.* **14**, 526-533, 627-636.

KATO, N. (1968). *J. Appl. Phys.* **39**, 2225-2230, 2231-2237.

KATO, N., USAMI, K. & KATAGAWA, T. (1967). *Adv. X-ray Anal.* **10**, 46.

KOHN, V. G. (1979*a*). *Phys. Status Solidi A*, **54**, 375-384.

KOHN, V. G. (1979*b*). *Kristallografiya*, **24**, 712-719.
KOZMIK, V. D. & MIKHAILYUK, I. P. (1978*a*). *Ukr. Fiz. Zh. (Ukr. Ed.)* **23**, 1570-1571.
KOZMIK, V. D. & MIKHAILYUK, I. P. (1978*b*). *Pis'ma Zh. Eksp. Teor. Fiz.* **28**, 673-674.
LEVONYAN, L. V. (1981). *Pis'ma Zh. Tech. Fiz.* **7**, 269-272.
PINSKER, Z. G. (1978). *Dynamical Scattering of X-rays in Crystals.* Heidelberg, New York: Springer-Verlag.
SUVOROV, E. V. & POLOVINKINA, V. I. (1974). *Pis'ma Zh. Eksp. Teor. Fiz.* **20**, 328-329.

Acta Cryst. (1986). A**42**, 435-441

The Intercomparison of Bragg X-ray Reflections from a Small Single Crystal – Zero-Wavelength-Dispersion Profile Measurement

BY A. MCL. MATHIESON* AND A. W. STEVENSON

Division of Chemical Physics, CSIRO, PO Box 160, *Clayton, Victoria, Australia* 3168

(*Received* 10 *December* 1985; *accepted* 21 *February* 1986)

Abstract

In conventional one-dimensional profile measurement procedures, either by diffractometry ('counter' profile) or by photography ('film' profile), intercomparison of Bragg reflections from a small single crystal, c, in a given experiment is rendered difficult, or impossible, by their wide variation in size with θ_c. Using synthetic $I(\Delta\omega, \Delta 2\theta)$ distributions, obtained by convolution of four components, the mosaic spread of the specimen crystal, μ, the emissivity distribution of the source, σ, its wavelength distribution, λ, and the detector aperture, δ, analysis shows how the 'counter' and 'film' profiles change with scan mode. In particular, it is shown that the 'film' profile obtained using an $\omega/2\theta$ ($s=2$) scan mode does not involve wavelength dispersion, so that the profile distribution can yield information about μ for each reflection and therefore about small differences in mosaic spread (and hence reflectivity) between reflections. Possible means of obtaining this profile using film or counter procedures are outlined.

Introduction

The intrinsic two-dimensional nature of the $\Delta\omega$, $\Delta 2\theta$ measurement procedure (Mathieson, 1982) and the detailed information which, with adequate resolution, it can yield, establishes it as a powerful means of investigating Bragg X-ray reflections from small single crystals. The 2D distribution can allow one to diagnose and estimate the individual linear distributions associated with the major components of the experiment, such as the mosaic-spread distribution of the specimen crystal, μ, the emissivity distribution of the X-ray source, σ, and its wavelength distribution, λ. With a minor experimental modification (Mathieson & Stevenson, 1984), the main components can be reduced to two, μ and λ, which can then be defined more precisely (Mathieson & Stevenson, 1985) so that variation of mosaic spread μ (*alias* reflectivity distribution, r - see Mathieson, 1984*a*) across a 60 μm crystal could be estimated (Mathieson & Stevenson, 1986).

Because the data are recorded in two dimensions, the $\Delta\omega, \Delta 2\theta$ measurement procedure is necessarily slower than one-dimensional procedures. It is, therefore, likely that, for reasons of convenience and speed, essentially one-dimensional procedures will continue to be used for routine data-collection tasks.

There is, however, no reason to assume, merely because of long-established usage, that the 1D procedures which are in current use necessarily supply either the best information or the available information in the best form. In this paper, we re-examine, from the $\Delta\omega, \Delta 2\theta$ viewpoint, the possibilities of 1D measurement - (*a*) to determine if there is any variant which would improve the quality of the 1D measurement and (*b*) to indicate possible advantageous ways of using position-sensitive detectors (p.s.d.'s) for 1D measurement when such detectors become available with sufficient spatial (angular) resolution.

Current one-dimensional procedures

In the currently conventional 1D measurement of Bragg X-ray reflections from a small single crystal, c, two main procedures are used. One involves a counter diffractometer using a wide aperture in front of the detector, the other uses photographic film. In attempting to compare reflections within a given experiment by either procedure, a basic difficulty results from the wide variation in the size of reflections. *Inter alia*, this feature complicates intrinsic problems in measurement, such as the distinction of what is peak and what is background, correction for thermal

* Present address: Department of Chemistry, La Trobe University, Bundoora, Victoria, Australia 3083.

0108-7673/86/060435-07$01.50